Supramolecular Hybrids of [60]Fullerene and Single-Wall Carbon Nanotubes

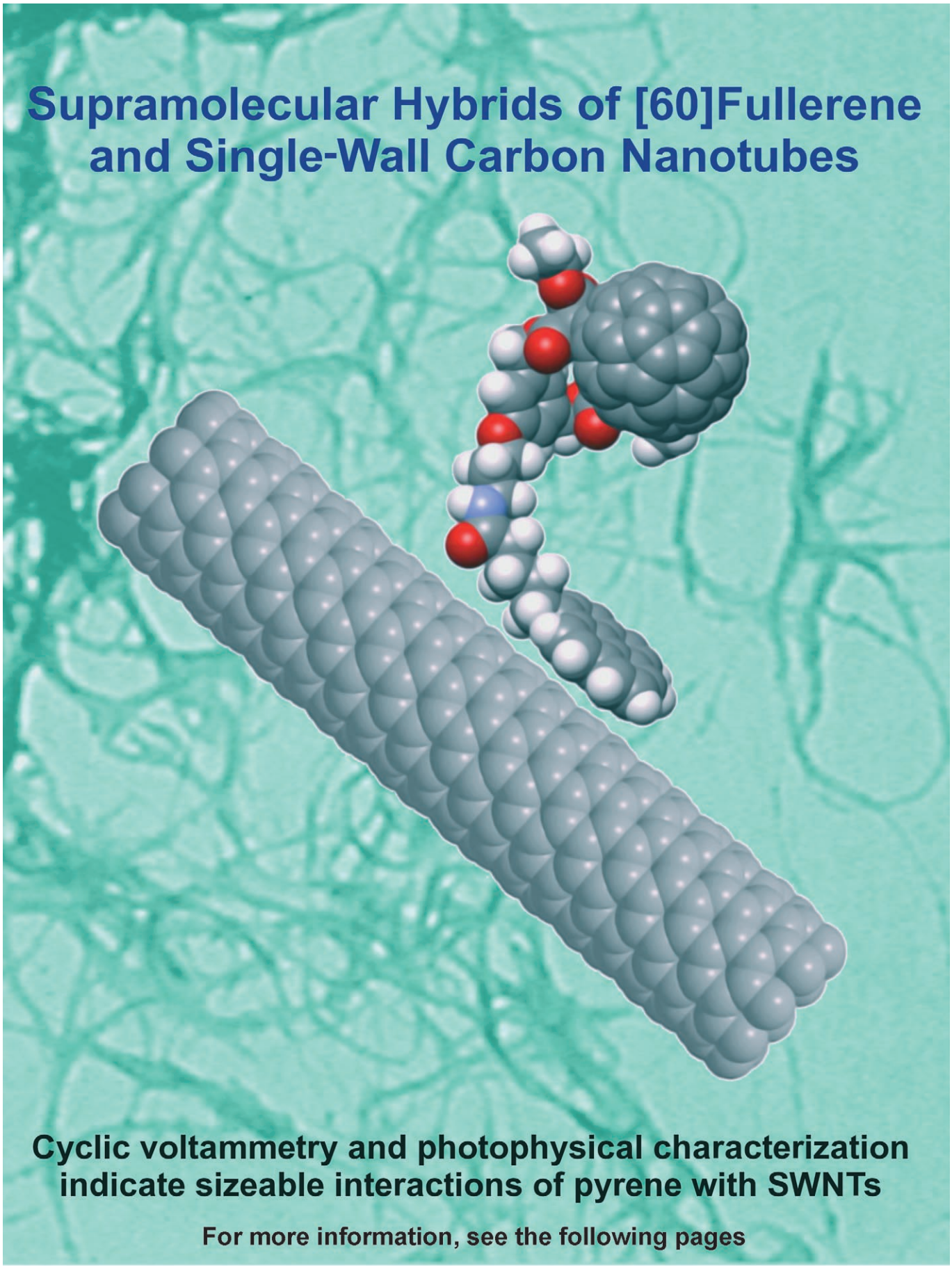

Cyclic voltammetry and photophysical characterization indicate sizeable interactions of pyrene with SWNTs

For more information, see the following pages

CHEMISTRY
A EUROPEAN JOURNAL

DOI: 10.1002/chem.200600114

Supramolecular Hybrids of [60]Fullerene and Single-Wall Carbon Nanotubes

Dirk M. Guldi,*[a] Enzo Menna,[b] Michele Maggini,*[b] Massimo Marcaccio,[c] Demis Paolucci,[c] Francesco Paolucci,*[c] Stéphane Campidelli,[d] Maurizio Prato,*[d] G. M. Aminur Rahman,[a] and Stefano Schergna[b]

Abstract: Noncovalent interactions between purified HiPCO single-wall carbon nanotubes (SWNT) and a [60]fullerene–pyrene dyad, synthesized through a regioselective double-cyclopropanation process, produce stable suspensions in which the tubes are very well dispersed, as evidenced by microscopy characterization. Cyclic voltammetry experiments and photophysical characterization of the suspensions in organic solvents are all indicative of sizeable interactions of the pyrene moiety with the SWNT and, therefore, of the prevalence in solution of [60]fullerene–pyrene·SWNT hybrids.

Keywords: carbon nanotubes · cyclic voltammetry · fullerenes · noncovalent interactions · supramolecular chemistry

Introduction

The intriguing properties of carbon nanostructures have sparked much interest in recent years, and a broad research effort has been dedicated to understanding the physical and physicochemical features of these new allotropes of carbon. Importantly, the wealth of information that has been gathered has significantly enhanced our general understanding of how to develop nanometer scale materials and devices that could shape future technologies.

[a] Prof. Dr. D. M. Guldi, Dr. G. M. A. Rahman
Lehrstuhl für Physikalische Chemie I
Universität Erlangen-Nürnberg
Egerlandstr. 3, 91058 Erlangen (Germany)
Fax: (+49) 9131-852-8307
E-mail: guldi@chemie.uni-erlangen.de

[b] Dr. E. Menna, Prof. M. Maggini, Dr. S. Schergna
INSTM, Unit of Padova, Dipartimento di Scienze Chimiche
Università di Padova, Via Marzolo 1, 35131 Padova (Italy)
Fax: (+39) 049-827-5239
E-mail: michele.maggini@unipd.it

[c] Dr. M. Marcaccio, Dr. D. Paolucci, Prof. F. Paolucci
INSTM, Unit of Bologna, Dipartimento di Chimica
Università di Bologna, Via Selmi 2, 40126 Bologna (Italy)
Fax: (+39) 051-209-9456
E-mail: francesco.paolucci@unibo.it

[d] Dr. S. Campidelli, Prof. M. Prato
INSTM, Unit of Trieste, Dipartimento di Scienze Farmaceutiche
Università di Trieste, Piazzale Europa 1, 34127 Trieste (Italy)
Fax: (+39) 040-52-572
E-mail: prato@units.it

In this context, carbon nanotubes (CNT), and in particular, single-wall carbon nanotubes (SWNT) have emerged as particularly attractive candidates, due to their outstanding physical, chemical, and mechanical properties, and their prospects for practical applications.[1] These systems consist of graphitic layers wrapped seamlessly into cylinders that originate from defined sections of two-dimensional graphene sheets.[2] With diameters of only a few nanometers and lengths of up to several centimeters, the length-to-width ratio of these nanotubes is extremely high. SWNT have a very broad range of electronic, thermal, and structural properties that vary according to the particular kind of SWNT. A setback in the use of CNT is that they are heavily entangled with one another, which leads to the formation of three-dimensional networks in the form of tightly bound bundles.[3]

To overcome the rather poor solubility of CNT in common solvents, it is desirable to develop facile, reproducible, and practical processing methods. Past work has unequivocally demonstrated that the preparation of functional CNT based nanocomposites (i.e., nanoconjugates and nanohybrids) requires a method that assists in disentangling and dispersing CNT.[4] However, it is evident that subsequent chemical and physical modification of the surface would be necessary to realize many of the potential applications.

Some SWNT have diameters that are sufficiently large to encapsulate various atoms and molecules into their one-dimensional nanocavity. So far, empty fullerenes,[5] endo-[6] and exohedral[7] metallofullerenes, exohedral fullerene derivatives,[8] single elements,[9] ionic salts,[10] alkali metal,[11] and H_2O[12] have been successfully incorporated into the

nanocavities of SWNT. Due to extensive intermolecular fullerene–fullerene or fullerene–SWNT interactions, it is expected that the physicochemical characteristics of these new materials are not simply a sum of those of fullerenes and nanotubes: this hypothesis was supported by several experimental and theoretical investigations.[13] Experimental results and theoretical studies demonstrate that the periodic array of [60]fullerene molecules gives rise to a hybrid electronic band that derives its character from both the SWNT states and the [60]fullerene molecular orbitals.[14]

Here we report on a new type of [60]fullerene-hybridized SWNT material, in which a covalently linked [60]fullerene–pyrene conjugate was immobilized onto the surface of SWNT by using a noncovalent method. The use of pyrene derivatives is crucial for our approach, namely, solubilization of SWNT through directed π–π interactions. A series of physicochemical probes (i.e., electrochemical, spectroscopic, and microscopic) confirm electronic interactions between the pyrene part of the [60]fullerene–pyrene conjugate and SWNT.

Results and Discussion

Synthesis of [60]fullerene–pyrene conjugate 1: The preparation of conjugate **1** began with the synthesis of [60]fullerene-substituted Boc-amine **6** (Boc = benzyloxycarbonyl, Scheme 1). This was obtained through the regioselective reaction developed by the group of F. Diederich,[15] which provides [60]fullerene bisadducts through a cyclization reaction at the [60]fullerene sphere by using bis malonates, in a double-cyclopropanation process. To this end, (3-bromopropyl)carbamic acid *tert*-butyl ester **3** and 3,5-bis(hydroxymethyl)phenol[16] were reacted in refluxing acetone in the presence of K_2CO_3 to afford bisdiol **4** in 91% yield.

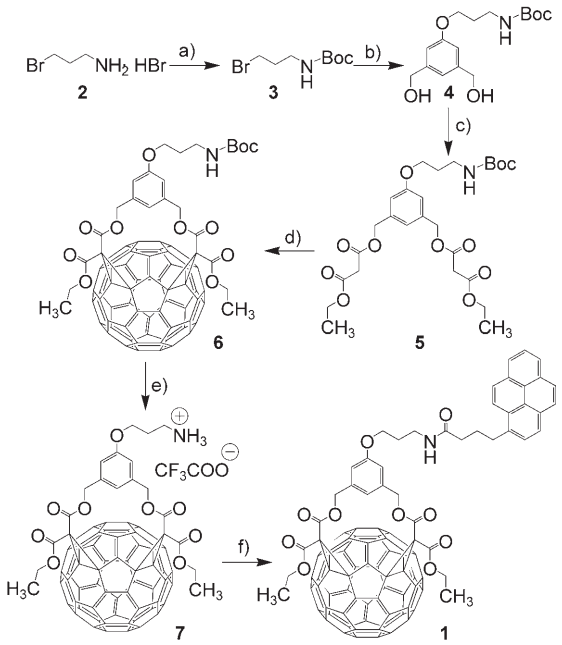

Scheme 1. a) $(BOC)_2O$, TEA, CH_2Cl_2; b) 3,5-bishydroxymethyl phenol, K_2CO_3, acetone; c) ethyl malonyl chloride, TEA, CH_2Cl_2; d) C_{60}, DBU, I_2, toluene; e) CF_3COOH, CH_2Cl_2; f) 1-pyrene butyric acid, HOBT, EDCI, 4-methylmorpholine (for abbreviations, see text).

Derivative **3** was, in turn, prepared from 3-bromopropyl amine hydrobromide **2**, as described in the literature.[17] Reaction of **4** with ethylmalonyl chloride in CH_2Cl_2 and triethylamine (TEA) gave bismalonate **5** in 56% yield. Treatment of **5** with [60]fullerene, I_2, and 1,8-diazabicyclo-[5.4.0]undec-7-ene (DBU) in toluene at room temperature afforded the cyclization product **6** in 46% yield. This was deprotected with trifluoroacetic acid in CH_2Cl_2 to yield derivative **7**, which was reacted with 1-pyrenebutyric acid, N-hydroxybenzotriazole (HOBT), 1-ethyl-3-(3′-dimethylaminopropyl)carbodiimide (EDCI), and 4-methylmorpholine to give the desired bisadduct **1** in 96% yield. The structure and purity of bisadduct **1** was confirmed by NMR spectroscopy and elemental analysis. In particular, the ^1H NMR spectrum of **1** shows all the characteristic features of the C_s-symmetrical 1,3-phenylenebis(methylene)-tethered fullerene *cis*-2 bisadduct subunit.[18] In fact, an AB quartet is observed for the diastereotopic benzylic $-CH_2-$ groups and two resonances are revealed for the aromatic protons of the 1,3,5-trisubstituted bridging phenyl ring. In addition to the signals corresponding to the [60]fullerene-substituted spacer, the resonances arising from the pyrene moiety are clearly observed between 7.5 and 8.5 ppm.

Binding of [60]fullerene–pyrene conjugate 1 to SWNT: The **1**·SWNT hybrids were prepared analogously to our previous work by using porphyrins (i.e., ZnP or H_2P).[4m] Stable dispersions of **1**·SWNT in organic solvents were achieved from a mixture of 1 mg of purified HiPCO (www.cnanotech.com) SWNT and 2 mg of **1** that was stirred for 24 h in 12 mL of DMF or THF. Sonication (Bransonic 52, 112 W) was carried out for 4 h at 20 °C followed by strong centrifugation (90 min at 10000 rpm). The excess **1** was removed by washing the deposit twice. In the final step, 12 mL of fresh solvent was added to the collected deposit and sonicated for 30 min at 20 °C. The solubility of **1**·SWNT at room temperature is 0.05 mg mL^{-1}. The homogeneous dispersion was stored at 4 °C for characterization. The black dispersion is stable in DMF for months and in THF for weeks.

Figure 1 shows a pictorial representation of hybrid **1**·SWNT, in which the optimized geometry of dyad **1** (at the PM3 semiempirical level) is shown with a (9,0) SWNT.

Electrochemical characterization: The electrochemical behavior of **1**·SWNT was investigated in both CH_2Cl_2 and THF, with tetrabutylammonium hexafluorophosphate (TBAH) as supporting electrolyte. Because the presence of high ionic concentrations may in principle alter the π–π stacking interactions between the SWNT and the pyrene moiety, the samples were sonicated only briefly (< 1 min) to facilitate the dispersion of **1**·SWNT in these solvents. Although similar results were observed for both solvents in the negative-potential region, the narrower positive-potential

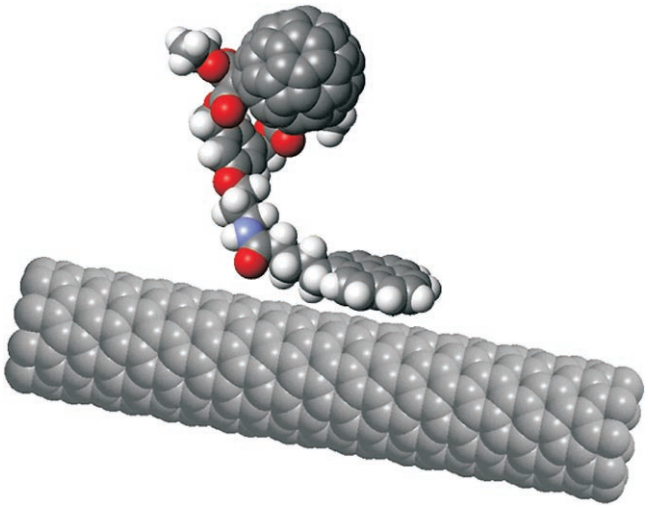

Figure 1. Semiempirical (PM3) optimized geometry of conjugate **1** in the presence of a (9,0) SWNT.

window that was available for THF prevented a thorough characterization of the anodic processes in THF.

The cyclic voltammetric (CV) curve for a saturated solution of **1**·SWNT in 0.05 M TBAH/CH_2Cl_2 (Figure 2, solid

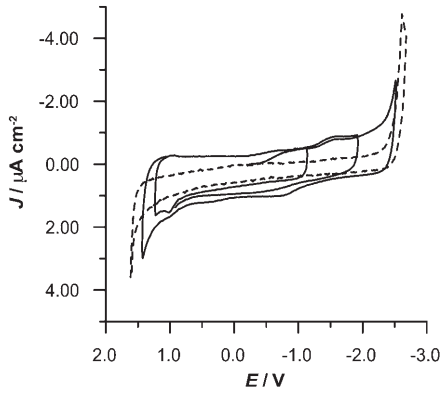

Figure 2. CV curves for a saturated solution of **1**·SWNT in 0.05 M TBAH/CH_2Cl_2 (solid line) and the corresponding baseline (dashed line). Data recorded at 298 K, scan rate 5 $V s^{-1}$. Working electrode, Pt disc (125 μm diameter). Potentials are referenced to the saturated calomel electrode (SCE).

line) displays the typical continuum of diffusion-controlled cathodic current, with onset at ~−0.45 V, which corresponds to the progressive filling of the empty electronic states of the SWNTs.[4j] Likewise, in the positive-potential region, the monotonic increase of anodic current is observed, with onset at ~+0.15 V and a sharp increase of current at $E=$ 1.3 V, also associated with the rise in the (filled) electronic density of state of SWNTs.[4j] Such behavior resembles closely that observed for other classes of functionalized SWNT, such as pyrrolidine-functionalized SWNTs,[4g] polystyrenesulfonate-[19] and poly(4-vinyl)pyridine-grafted SWNTs.[20] Superimposed to such a continuum of faradaic and pseudocapacitive current, the CV curve in Figure 2 also displays three discrete peaks, at −0.79, −1.58, and +0.98 V that, by comparison with model **1**, were associated with redox processes involving the fullerene moiety. The CV curve of the latter species, obtained under similar conditions (Figure 3), displays in fact two reduction peaks, denoted as I and II, at −0.74 and −1.12 V, respectively, and an oxidation peak at 1.19 V (peak A).

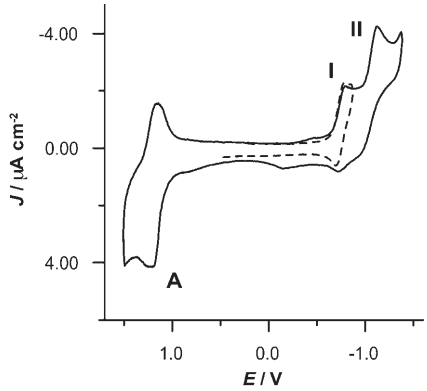

Figure 3. CV curves for a 0.3 mM solution of conjugate **1** in 0.05 M TBAH/CH_2Cl_2. Data recorded at 298 K, scan rate 5 $V s^{-1}$. Working electrode, Pt disc (125 μm diameter). Potentials are referenced to SCE.

Noticeably, peak I in the CV curve of model species is reversible and corresponds to a one-electron reduction, whereas peak II is irreversible most likely because of follow-up reactions associated with electrochemically induced opening of the cyclopropane ring(s), as typically observed in malonate-fullerenes.[21] Importantly, the anodic peak at 1.19 V in the CV curve of **1** corresponds to a two-electron oxidation process (by comparison with the first reduction of the fullerene moiety) that results from the superimposition of two one-electron oxidations, occurring at very close potentials, as evidenced in the CV curve at low temperature shown in Figure 4. The corresponding $E_{1/2}$ values, as obtained by the

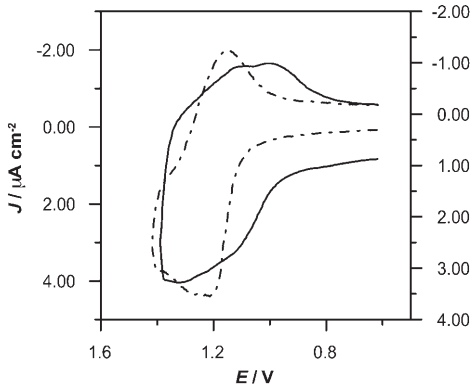

Figure 4. CV curves for a 0.3 mM solution of conjugate **1** in 0.05 M TBAH/CH_2Cl_2. Data collected at: 1 $V s^{-1}$ and 298 K (dashed line); 10 $V s^{-1}$ and 223 K (solid line). Working electrode. Pt disc (125 μm diameter). Solid line is referred to the right *y* axis, the dashed line to the left *y* axis. Potentials are referenced to SCE.

digital simulation of the CV curves, were 1.15 and 1.22 V, respectively.

The anodic behavior of fullerenes and fullerene derivatives has received much less attention than the corresponding cathodic behavior.[22] However, potentials ranging between 1.2 and 1.4 V have been reported for the first oxidation of bisadducts that are structurally closely related to **1**.[23] One of the two one-electron oxidation processes comprising peak A is, therefore, attributed to the oxidation of the fullerene moiety, the remaining process being located on the pyrene moiety.[24]

Comparison of the CV curves of **1**·SWNT and **1** (Figure 5) highlighted, besides the typical features due to the SWNT

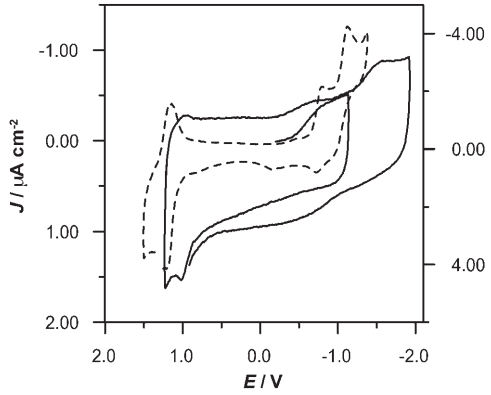

Figure 5. CV curves for a 0.05 M TBAH/CH_2Cl_2 solution of saturated **1**·SWNT (solid line) and 0.3 mM **1** (dashed line). Data recorded at 298 K, scan rate 5 $V s^{-1}$. Working electrode, Pt disc (125 μm diameter). Solid line is referred to the left *y* axis, the dashed line to the right *y* axis. Potentials are referenced to SCE.

moiety as described above, significant changes in the redox properties of the fullerene derivative. A general broadening of the voltammetric peaks is observed with respect to the model. This may be attributed to joint mass-transport and charge-transfer kinetics effects derived from association of **1** to the SWNT: both a smaller diffusion coefficient and hindering of electronic interaction between the fullerene derivative and the electrode surface might, in fact, explain the overall change in the CV morphology of **1** upon association with the SWNT. Importantly, a dramatic change in the anodic behavior of the fullerene derivative was observed upon its interaction with SWNT: the oxidation peak at 0.98 V in the CV curve of **1**·SWNT contrasts with peak A of **1** because 1) it involves only one electron (compared to two electrons for **1**) and 2) it is shifted relative to **1** by about 200 mV towards less-positive potentials. Both effects may be ascribed to the electronic interaction of pyrene with the SWNT π-system that would, as observed recently in a similar system,[25] make oxidation of the pyrene moiety easier. In particular, the measured negative shift of 200 mV of the pyrene$^+$/pyrene redox potential would correspond to an ~20 $kJ mol^{-1}$ stabilization of the pyrene radical cation by its interaction with the SWNT. By contrast, the fullerene-centered oxidation, occurring in **1** close to the pyrene-centered oxidation, would not be affected significantly by such an interaction, and would, therefore, remain at more-positive potentials (i.e., ≥1.2 V), at which the CV curve is dominated by the increase in the anodic current associated with the oxidation of SWNT.

Photophysical characterization: Absorption spectroscopy (Figure 6) also confirms the successful immobilization of **1**

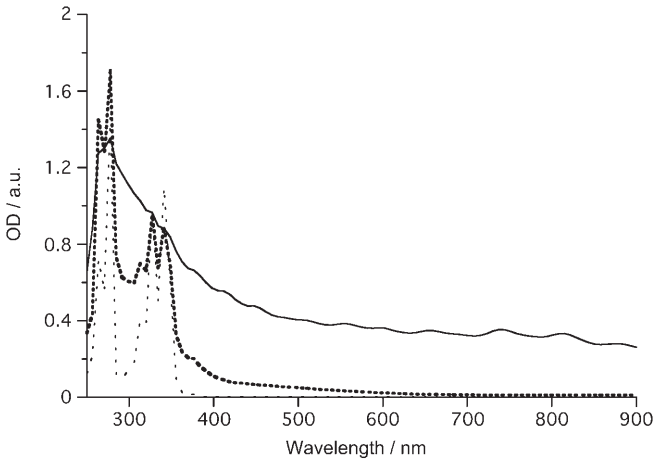

Figure 6. Absorption spectra of 1-pyrenemethanol (dotted line), dyad **1** (dashed line), and **1**·SWNT (solid line) in DMF at RT.

onto the SWNT surface. In particular, the spectrum of **1** is dominated by the UV characteristics of pyrene with a set of maxima at 265, 277, 300, 313, 328, and 345 nm, whereas the [60]fullerene transitions appear only as an overall broadening. The broadening starts essentially in the UV region and tails out in the visible region. Relative to a pyrene reference (i.e., 1-pyrenemethanol) no significant perturbation of the absorption characteristics are seen. This finding corroborates the lack of substantial electronic interactions between the two π-systems in **1**. For a suspension of **1**·SWNT, apart from the pyrene features, the characteristic van Hove singularities of SWNT are discernable in the visible/near-IR region up to 360 nm, and the π–π* transition of pyrene dominates the spectrum. Collectively, these observations confirm the presence of both constituents, SWNT and **1**, in the form of a novel π-complex.

Additional proof for **1**·SWNT interactions came from fluorescence data. However, the photoreactivity of **1** should be discussed first (Figure 7).

In line with previous reports, the photoreactivity of such hybrids is dominated by the intramolecular transduction of singlet excited-state energy.[26] Relative to 1-pyrenemethanol (fluorescence quantum yield = 0.1), strong pyrene fluorescence (375, 385, 395, and 418 nm) quenching (fluorescence quantum yield = 0.03) in the UV-visible region is linked to an activation of [60]fullerene fluorescence (698 nm) in the visible/near-IR region (i.e., ~3×10^{-4}). In **1**, an excitation spectrum of [60]fullerene fluorescence tracks the pyrene ab-

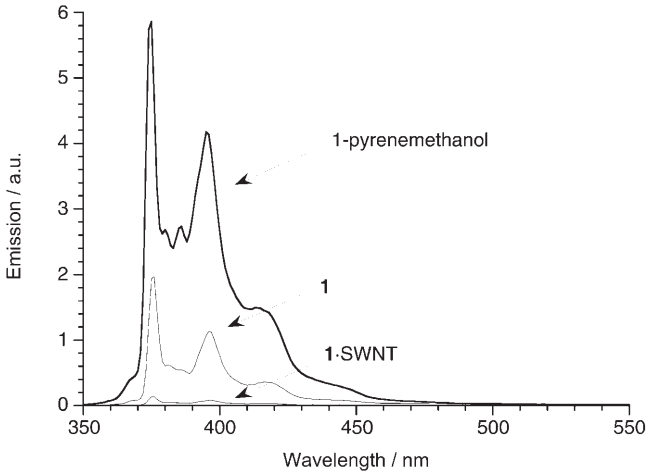

Figure 7. RT fluorescence spectra of 1-pyrenemethanol, derivative **1**, and **1**·SWNT in DMF with matching absorption, similar to that shown in Figure 6, at the 329 nm excitation wavelength.

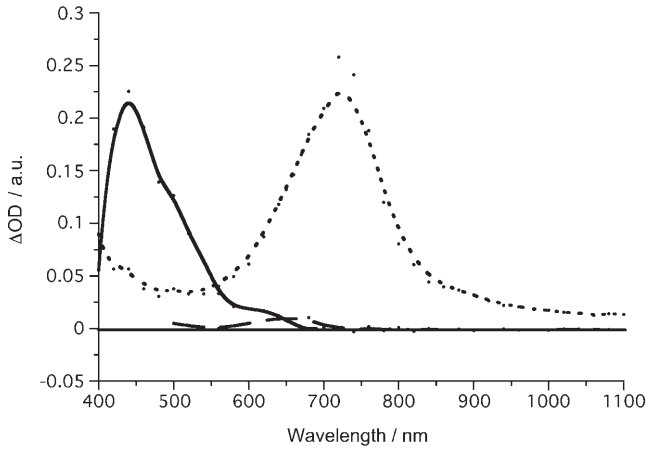

Figure 8. Differential absorption spectrum (visible and near-IR) obtained upon nanosecond flash photolysis (355 nm) of 1-pyrenemethanol (solid line), conjugate **1** (dashed line) and **1**·SWNT (dotted line) in nitrogen-saturated DMF with a 50 ns time delay at RT.

sorption spectrum and, hence, validates the energy-transfer process. The less-than-unity efficiency for the intramolecular singlet–singlet energy transfer could be rationalized by sizeable donor–acceptor separation ranging from 10 to about 17 Å because of the conformational freedom of the alkyl spacer between the [60]fullerene and pyrene moieties. The corresponding **1**·SWNT photoexcitation into the pyrene π–π* transition at 328 nm results in 1) a further ~7-fold quenching of the pyrene-centered fluorescence (i.e., 4×10^{-3}) and 2) a nearly complete elimination of the [60]fullerene-centered fluorescence (i.e., $<3\times10^{-5}$). Such behavior indicates a competitive deactivation—SWNT versus [60]fullerene—of the pyrene singlet-excited state. In this context, it is important to note that pyrene, which is either surface-immobilized onto SWNT (i.e., noncovalent π–π interactions) or linked to SWNT (i.e., covalent spacers), gives rise to strong fluorescence quenching. In other words, the fluorescence of pyrene and [60]fullerene are excellent probes for detecting electronic interactions between SWNT and pyrene.

Similarly, in time-resolved fluorescence experiments we found that the long-lived pyrene π–π* fluorescence lifetime (~50 ns) is shortened in **1** (17 ns), whereas that of [60]fullerene remains at 1.5 ± 0.2 ns, essentially unchanged relative to appropriate [60]fullerene references. On the other hand, in **1**·SWNT, SWNT-induced deactivation of the pyrene fluorescence could not be detected within the instrumental time resolution of our apparatus (i.e., 100 ps).

For independent confirmation of the electronic interactions we used nanosecond transient spectroscopy with photoexcitation at 337 nm, which corresponds to a wavelength of predominant pyrene absorption (i.e., >95%). In line with our fluorescence-based conclusion, the only discernable features in conjugate **1** are those of the long-lived [60]fullerene triplet, that is, a transient maximum at around 700 nm[27] (Figure 8).

The triplet–triplet absorptions of pyrene, which are seen for 1-pyrenemethanol at around 420 nm, are entirely lacking in **1**, regardless of the time delay. The [60]fullerene triplet converts slowly to the ground state with lifetimes that are typically around 20 μs. Such reactivity is found in nonpolar toluene, medium-polar THF, and polar DMF. In contrast, upon probing **1**·SWNT no appreciable features are seen at all on the nanosecond scale. This again attests to SWNT-induced processes that compete with [60]fullerene in the excited-state deactivation of pyrene.

Microscopic characterization: Transmission electron microscopy (TEM) confirmed the presence of SWNT in our sample. Two representative images, shown in Figure 9, reveal high aspect-ratio objects that appear throughout the scanned regions. The mean length of these objects is typically on the order of several microns, and their diameters range between a few nanometers and several tens of nanometers. Notably, Figure 9b shows very well-dispersed SWNT. In this regard, **1**·SWNT is different from pristine HiPCO SWNT, in which aggregation prevents the observation of individual SWNTs or very thin bundles.

We also investigated **1**·SWNT by atomic force microscopy (AFM). The sample was prepared by spin coating on a silicon wafer from a DMF solution and revealed the coexistence of individual SWNT (diameters of around 1.2 nm) of several hundred nanometers in length (Figure 10) and well-dispersed thin bundles of SWNT. However, we failed to confirm microscopically the presence of fullerene moieties on the SWNT sidewalls. Considering that these AFM pictures are virtually identical to those obtained upon dispersing SWNT with amphiphilic pyrene derivatives,[28] the current homogeneous dispersions are consistent with surface-immobilization of **1**.

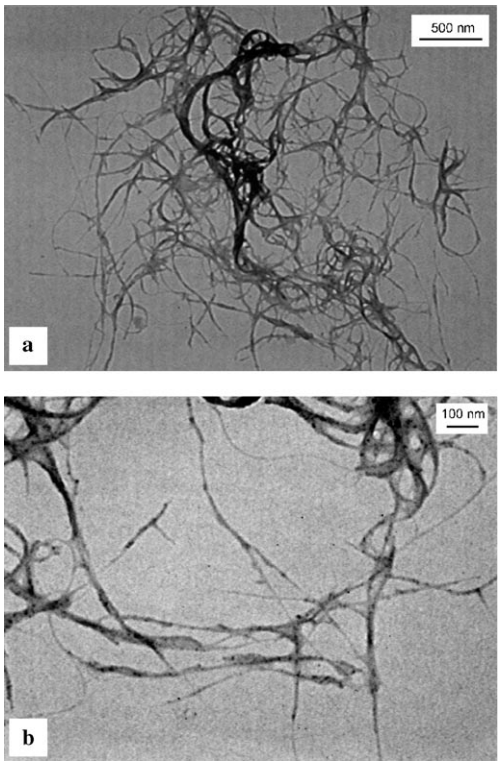

Figure 9. TEM images of **1**·SWNT from a DMF solution.

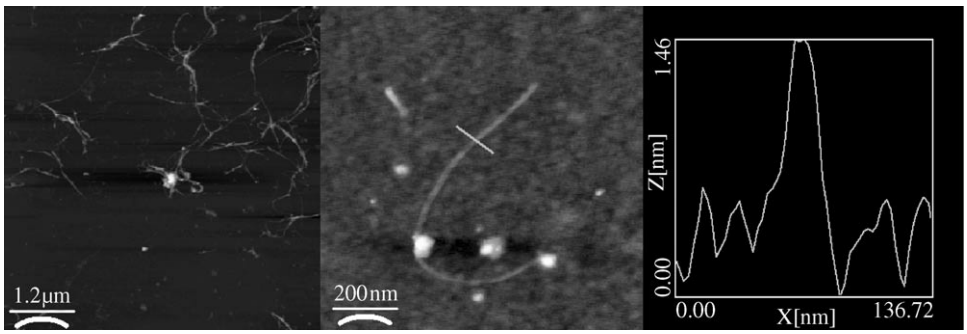

Figure 10. AFM images of **1**·SWNT on silicon wafer. The images show the small bundles of nanotubes (left) and an individual tube (middle). The picture on the right indicates the diameter of the single nanotube.

Conclusion

We have shown that [60]fullerene–pyrene conjugate **1** enabled the homogeneous dispersion of purified HiPCO SWNT in organic solvents. Cyclic voltammetry experiments and photophysical and microscopic characterization of the dispersed material supports the view that π–π interactions between SWNT and the pyrene moiety govern the association of **1** with the sidewalls of SWNT, although we were unable to visualize individual fullerene moieties by appropriate TEM analysis. In particular, the measured 200 mV positive shift of pyrene^{+}/pyrene redox potential is indicative of a direct electronic interaction of pyrene with the SWNT π-system. This conclusion was corroborated by nanosecond transient spectroscopy that showed competition between SWNT-induced processes and [60]fullerene in the excited-state deactivation of pyrene. Use of this nanoscale system for applications in photovoltaics and molecular electronics is currently underway.

Experimental Section

Materials: [60]Fullerene was purchased from Bucky USA (99.5%), HiPCO SWNT was from CNI (www.cnanotech.com). 1-Pyrenebutyric acid and all other reagents were used as purchased from Sigma-Aldrich and Fluka. CH_2Cl_2, THF, and DMF employed for UV/Vis and fluorescence measurements were spectrophotometric-grade solvents. Solvents employed for electrochemical measurements (CH_2Cl_2 purum, Fluka and THF, LiChrosolv, Merck) were treated according to procedures described elsewhere.[22,29] 3,5-Bis(hydroxymethyl)phenol[16] and derivative **2**[17] were prepared as previously described. Tetrabutylammonium hexafluorophosphate (TBAH, puriss., Fluka) was used as supporting electrolyte as received. The original suspension of **1**·SWNT in THF was dried firstly under an argon flow to give a black powder that was dispersed in CH_2Cl_2 and used for the electrochemical characterization.

Instrumentation: Column chromatography was performed by using silica gel MN 60 (70–230 Mesh) from Macherey-Nagel. ^{1}H (250.1 MHz) and ^{13}C (62.9 MHz) NMR spectra were recorded by using a Bruker AC-F 250 spectrometer. The ESI-MS spectra were recorded by using a Thermo Finnigan AQA LC/MS: spray voltage −4 kV; capillary voltage −10 V; capillary temperature 180 °C; nitrogen as nebulizing gas. The samples were dissolved in methanol containing 1% trifluoroacetic acid. Elemental analyses were provided by the facility at the Department of Chemical Sciences at the University of Padova. Nanosecond laser flash photolysis experiments were performed by using a Quanta-Ray CDR Nd:YAG system (6 ns pulse width) in a front-face excitation geometry. Fluorescence lifetimes were measured by using a laser strope fluorescence lifetime spectrometer (Photon Technology International) with 337 nm laser pulses from a nitrogen laser fiber coupled to a lens-based T-formal sample compartment equipped with a stroboscopic detector. Emission spectra were recorded by using a FluoroMax-3 (Horiba Company). The experiments were performed at RT. The cyclic voltammetry experiments were performed in a one-compartment electrochemical cell of airtight design, with high-vacuum glass stopcocks fitted with either Teflon or Viton (DuPont) O-rings to prevent contamination by grease. The connections to the high-vacuum line and to the Schlenk tube containing the solvent were obtained by spherical joints also fitted with Teflon O-rings. The cell, containing the supporting electrolyte and the electroactive compound, was dried under vacuum at 363 K for at least 48 h. Afterwards, the solvent was distilled by a trap-to-trap procedure into the electrochemical cell just prior to performing the electrochemical experiment. The pressure measured in the electrochemical cell prior to performing the trap-to-trap distillation of the solvent was typically $(1.0–2.0)\times 10^{-5}$ mbar. The working electrode was a Pt disc ultramicroelectrode (diameter, 125 μm) sealed in glass. The counterelectrode consisted of a platinum spiral, and the quasireference electrode was a silver spiral. The quasireference electrode drift was negligible for the time required by a single experiment. Both the counter and the reference electrodes were separated from the working electrode by ~0.5 cm. Potentials were measured with respect to the decamethylferrocene standard. $E_{1/2}$ values correspond

to $(E_{pc}+E_{pa})/2$ from CV. Voltammograms were recorded by using a home-made fast potentiostat controlled by an AMEL Model 568 function generator. Data acquisition was performed by using a Nicolet Model 3091 digital oscilloscope interfaced to a PC. Digital simulations of the cyclic voltammetric curves were conducted by using the DigiSim 3.0 software by Bioanalytical Systems.

Bisdiol 4: K_2CO_3 (1.5 g, 15.3 mmol) was added to a solution of derivative **2** (804.4 mg, 3.4 mmol) and 3,5-bis(hydroxymethyl)phenol (520.0 mg, 3.4 mmol) in acetone (100 mL), and the suspension was kept overnight at reflux temperature. After cooling to RT, the salts were filtered and washed with cold ethanol. The filtrate was evaporated under reduced pressure and the residue, dissolved in $CHCl_3$ (50 mL), was washed with water (2×35 mL). The organic phase, dried over $MgSO_4$, was concentrated under reduced pressure to give 960 mg (91%) of **4** as a clear, yellow oil. ^{1}H NMR (250 MHz, $CDCl_3$, 25°C, TMS): $\delta=6.90$ (s, 1H; Ph), 6.81 (s, 2H; Ph), 4.64 (s, 2H; OH), 4.62 (s, 4H; CH_2), 4.00 (t, ^3J(H,H)=5.8 Hz, 2H; CH_2), 3.27 (m, 2H; CH_2), 1.94 (m, 2H; CH_2), 1.42 ppm (s, 9H; CH_3); ^{13}C NMR (62.9 MHz, $CDCl_3$, 25°C, TMS): $\delta=158.90$, 142.78, 118.30, 117.49, 111.77, 64.46, 64.38, 30.80, 29.36, 28.29, 27.57 ppm; IR (KBr): $\tilde{\nu}=3350$, 2976, 2932, 2874, 1756, 1688, 1597, 1523, 1453, 1391, 1366, 1250, 1164, 1055, 911, 850, 779, 731 cm^{-1}; ESI-MS: m/z: 334 $[M+Na]^+$.

Bismalonate 5: Ethyl malonyl chloride (416.0 µl, 3.70 mmol), previously dissolved in CH_2Cl_2 (25 mL), was slowly added at 0°C to a solution of **4** (460.0 mg, 1.48 mmol) and TEA (515.0 µL, 3.70 mmol) in CH_2Cl_2 (75 mL). The solution was allowed to warm to RT over a period of 30 min, and was then stirred at that temperature for 4 h. The mixture was washed with a saturated aqueous $NaHCO_3$ solution (2×30 mL), then with water (2×50 mL), dried over $MgSO_4$, and concentrated under reduced pressure. The crude product was purified by flash column chromatography (SiO_2, eluent: $CHCl_3$ and then $CHCl_3$/MeOH 9:1) affording 447 mg (56%) of **5** as a clear oil. ^{1}H NMR (250 MHz, $CDCl_3$, 25°C, TMS): $\delta=6.90$ (s, 1H; Ph), 6.84 (s, 2H; Ph), 5.12 (s, 4H; CH_2), 4.19 (q, ^3J(H,H)=7.1 Hz, 4H; CH_2), 4.01 (t, ^3J(H,H)=5.8 Hz, 2H; CH_2), 3.41 (s, 4H; CH_2), 3.30 (m, 2H; CH_2), 1.43 (s, 9H; CH_3), 1.27 ppm (t, ^3J(H,H)=7.1 Hz, 6H; CH_3); ^{13}C NMR (62.9 MHz, $CDCl_3$, 25°C, TMS): $\delta=166.31$, 159.15, 155.93, 137.15, 119.92, 114.04, 66.60, 61.56, 41.48, 28.35, 13.98 ppm; IR (KBr): $\tilde{\nu}=3403$, 2979, 2939, 1733, 1600, 1515, 1458, 1367, 1331, 1299, 1250, 1032, 852, 777, 713, 685 cm^{-1}; ESI-MS: m/z: 540 $[M]^+$ and 563 $[M+Na]^+$.

[60]Fullerene bisadduct 6: DBU (622.0 µl, 4.17 mmol) was added at RT to a solution of [60]fullerene (500 mg, 0.69 mmol), I_2 (353.0 mg, 1.39 mmol), and bismalonate **5** (371 mg, 0.69 mmol) in toluene (500 mL). The solution was stirred at that temperature for 3 h, then concentrated under reduced pressure. The crude product was purified by flash column chromatography (SiO_2, eluent: toluene then toluene/AcOEt 7:3) and crystallized from $CHCl_3$/hexane affording 400 mg (46%) of **6** as a dark-red solid. ^{1}H NMR (250 MHz, $CDCl_3$, 25°C, TMS): $\delta=7.12$ (s, 1H; Ph), 6.80 (s, 2H; Ph), 5.80 (d, $^2J=12.8$ Hz, 2H; CH_2), 5.14 (d, $^2J=12.8$ Hz, 2H; CH_2), 4.60–4.20 (m, 4H; CH_2), 4.07 (t, ^3J(H,H)=5.8 Hz, 2H; CH_2), 3.33 (m, 2H; CH_2), 2.00 (m, 2H; CH_2), 1.46 (s, 9H; CH_3), 1.36 ppm (t, ^3J(H,H)=7.1 Hz, 6H; CH_3); ^{13}C NMR (62.9 MHz, $CDCl_3$, 25°C, TMS): $\delta=162.91$, 162.82, 158.87, 148.72, 147.55, 147.50, 147.34, 146.12, 146.09, 145.77, 145.66, 14538, 145.21, 145.06, 144.62, 144.28, 144.19, 143.99, 143.78, 143.61, 143.30, 143.28, 143.06, 142.33, 141.27, 141.06, 139.97, 138.12, 136.27, 135.87, 129.00, 128.53, 128.20, 115.36, 112.35, 70.65, 67.27, 63.34, 31.55, 28.41, 22.63, 14.14, 14.10 ppm; IR (KBr): $\tilde{\nu}=3431$, 2973, 1748, 1715, 1600, 1502, 1460, 1365, 1460, 1365, 1328, 1297, 1233, 1206, 1168, 1101, 1057, 1018, 859, 732, 702, 549, 525 cm^{-1}; UV/Vis (CH_2Cl_2): λ_{max} (ε)=210.4 (61331), 218.4 (67553), 231.2 (121487), 256.8 nm (144807 mol^{-1} m^3 cm^{-1}); elemental analysis calcd (%) for $C_{68}H_{17}NO_3$ (896): C 91.17, H 1.91, N 1.56; found: C 90.43, H 1.97, N 1.60.

[60]Fullerene derivative 7: A solution of bisadduct **6** (200 mg, 0.16 mmol) and trifluoroacetic acid (2.5 mL, 0.03 mmol) in dry CH_2Cl_2 (50 mL) was stirred at RT for 30 min. The mixture was concentrated under reduced pressure to afford the unprotected product **7** as a brownish powder in nearly quantitative yield. The crude product was used for the next step without further purification.

[60]Fullerene–pyrene dyad 1: A solution of HOBT (12.8 mg, 0.09 mmol), EDCI (18.1 mg, 0.09 mmol), and 1-pyrene butyric acid (25.0 mg, 0.09 mmol) in CH_2Cl_2 (50 mL) was stirred for 15 min and then added dropwise to a suspension of **7** (100.0 mg, 0.08 mmol) and 4-methylmorpholine (10.4 µl, 0.09 mmol) in CH_2Cl_2 (15 mL) at 0°C. After 20 min, the mixture was washed with water (2×20 mL), dried over $MgSO_4$, and concentrated under reduced pressure. The crude product was purified by flash column chromatography (SiO_2, eluent: toluene/AcOEt/MeOH 5:4:1) affording 108 mg (96%) of **1** as a brown-red solid material. ^{1}H NMR (250 MHz, $CDCl_3$, 25°C, TMS): $\delta=8.40$–7.80 (m, 9H; Ph), 7.10 (s, 1H; Ph), 6.71 (s, 2H; Ph), 5.72 (brs, 1H; NH), 5.67 (d, ^2J(H,H)=12.8 Hz, 2H; CH_2), 5.07 (d, ^2J(H,H)=12.8 Hz, 2H; CH_2), 4.60–4.30 (m, 4H; CH_2), 4.01 (t, ^3J(H,H)=5.8 Hz, 2H; CH_2), 3.50–3.30 (m, 4H; CH_2), 2.40–2.10 (m, 4H; CH_2), 1.99 (m, 2H; CH_2), 1.35 ppm (t, ^3J(H,H)=7.1 Hz, 6H; CH_3); ^{13}C NMR (62.9 MHz, $CDCl_3$, 25°C, TMS): $\delta=177.78$, 172.92, 162.85, 158.638, 145.99, 145.69, 145.66, 145.59, 145.30, 145.15, 145.00, 144.53, 144.36, 144.24, 144.12, 143.90, 143.69, 143.50, 143.25, 143.00, 142.18, 141.22, 141.00, 139.87, 138.17, 137.49, 136.19, 135.83, 135.73, 135.52, 134.67, 131.36, 130.84, 129.96, 129.92, 128.74, 128.70, 127.45, 127.39, 127.32, 126.73, 126.70, 125.86, 125.82, 125.05, 124.93, 124.89, 124.79, 123.32, 123.23, 115.42, 112.27, 70.60, 67.24, 66.21, 63.27, 49.18, 36.05, 32.66, 30.92, 27.35, 14.16 ppm; IR (KBr): $\tilde{\nu}=3426$, 2973, 1747, 1671, 1600, 1509, 1460, 1368, 1328, 1297, 1233, 1207, 1170, 1099, 1057, 1018, 843, 704, 549, 525 cm^{-1}; UV/Vis (CH_2Cl_2): λ_{max} (ε)=220.0 (114463), 234.4 (263371), 244.0 (323675), 265.6 (232328), 276.8 (236551), 313.6 (84216), 328.0 (116411), 344.0 (132947 mol^{-1} m^3 cm^{-1}); elemental analysis calcd (%) for $C_{101}H_{39}NO_{10}$ (1426): C 85.05, H 2.76, N 0.98; found: C 82.77, H 2.50, N 0.91.

Acknowledgements

Funding from MIUR (GR/No. PRIN2004035502, RBAU017S8R, RBNE01P4JF, RBNE019NKS, RBNE033KMA), ITM-CNR, the European Union (TRN network WONDERFULL), the Deutsche Forschungsgemeinschaft (SFB 583), FCI, and the Office of Basic Energy Sciences of the U.S. Department of Energy are gratefully acknowledged.

[1] a) M. J. O'Connel, S. M. Bachilo, C. B. Huffmann, V. C. Moore, M. S. Strano, E. H. Haroz, K. L. Rialon, P. J. Boul, W. H. Noon, C. Kittrell, J. Ma, R. H. Hauge, R. B. Weisman, R. E. Smalley, *Science* **2002**, *297*, 593; b) M. S. Dresselhaus, G. Dresselhaus, P. C. Eklund, *Science of Fullerenes and Carbon Nanotubes*, Academic Press, New York, **1996**; c) A. C. Dillon, T. Gennet, K. M. Jones, J. L. Alleman, P. A. Parilla, M. J. Heben, *Adv. Mater.* **1999**, *11*, 1354; d) S. Paulson, A. Helsen, N. M. Buongiorno, R. M. Taylor, M. Falvo, R. Superfine, S. Washburn, *Science* **2000**, *290*, 1742; e) L. Sun, R. M. Crooks, *J. Am. Chem. Soc.* **2000**, *122*, 12340; f) B. Z. Tang, H. Xu, *Macromolecules* **1999**, *32*, 2569; g) P. M. Ajayan, O. Zhou in *Carbon Nanotubes: Synthesis, Structure, Properties, and Applications, Vol. 80* (Eds.: M. S. Dresselhaus, G. Dresselhaus, P. Avouries), Springer-Verlag, Heidelberg, **2001**; h) A. Hirsch, *Angew. Chem.* **2002**, *114*, 1933; *Angew. Chem. Int. Ed.* **2002**, *41*, 1853; i) D. Tasis, N. Tagmatarchis, V. Georgakilas, M. Prato, *Chem. Eur. J.* **2003**, *9*, 4000; j) P. M. Ajayan, *Chem. Rev.* **1999**, *99*, 1787.

[2] a) H. J. Dai, *Acc. Chem. Res.* **2002**, *35*, 1035; b) J. T. Hu, T. W. Odom, C. M. Lieber, *Acc. Chem. Res.* **1999**, *32*, 435; c) B. Vigolo, A. Penicaud, C. Coulon, C. Sauder, R. Pailler, C. Journet, P. Bernier, P. Poulin, *Science* **2000**, *290*, 1331; d) M. Ouyang, J.-L. Huang, C. M. Liber, *Acc. Chem. Res.* **2002**, *35*, 1035.

[3] a) P. M. Ajayan, L. S. Schadler, C. Giannaris, A. Rubio, *Adv. Mater.* **2000**, *12*, 750; b) R. J. Chen, Y. Zhang, D. Wang, H. Dai, *J. Am. Chem. Soc.* **2001**, *123*, 3838; c) R. Bandyopadhyaya, E. Nativ-Roth, O. Regev, R. Yerushalmi-Rozen, *Nano Lett.* **2002**, *2*, 25; d) P. Avouris, *Acc. Chem. Res.* **2002**, *35*, 1026.

[4] a) V. Georgakilas, K. Kordatos, M. Prato, D. M. Guldi, M. Holzinger, A. Hirsch, *J. Am. Chem. Soc.* **2002**, *124*, 760; b) Y.-P. Sun, K. Fu,

Y. Lin, W. Huang, *Acc. Chem. Res.* **2002**, *35*, 1096; c) D. M. Guldi, G. M. A. Rahman, F. Zerbetto, M. Prato, *Acc. Chem. Res.* **2005**, *38*, 871; d) N. Tagmatarchis, M. Prato, *J. Mater. Chem.* **2004**, *14*, 437; e) C. A. Dyke, J. M. Tour, *Chem. Eur. J.* **2004**, *10*, 812; f) V. Georgakilas, D. Voulgaris, E. Vázquez, M. Prato, D. M. Guldi, A. Kukovecz, H. Kuzmany, *J. Am. Chem. Soc.* **2002**, *124*, 14318; g) D. M. Guldi, M. Marcaccio, D. Paolucci, F. Paolucci, N. Tagmatarchis, D. Tasis, E. Vázquez, M. Prato, *Angew. Chem.* **2003**, *115*, 4338; *Angew. Chem. Int. Ed.* **2003**, *42*, 4206; h) D. M. Guldi, M. Holzinger, A. Hirsch, V. Georgakilas, M. Prato, *Chem. Commun.* **2003**, 1130; i) V. Georgakilas, N. Tagmatarchis, D. Pantarotto, A. Bianco, J.-P. Briand, M. Prato, *Chem. Commun.* **2002**, 3050; j) M. Melle-Franco, M. Marcaccio, D. Paolucci, F. Paolucci, V. Georgakilas, D. M. Guldi, M. Prato, F. Zerbetto, *J. Am. Chem. Soc.* **2004**, *126*, 1646; k) G. M. A. Rahman, D. M. Guldi, R. Cagnoli, A. Mucci, L. Schenetti, L. Vaccari, M. Prato, *J. Am. Chem. Soc.* **2005**, *127*, 10051; l) D. M. Guldi, G. M. A. Rahman, M. Prato, N. Jux, S. Qin, W. Ford, *Angew. Chem.* **2005**, *117*, 2051; *Angew. Chem. Int. Ed.* **2005**, *44*, 2015; m) D. M. Guldi, G. M. A. Rahman, N. Jux, N. Tagmatarchis, M. Prato, *Angew. Chem.* **2004**, *116*, 5642; *Angew. Chem. Int. Ed.* **2004**, *43*, 5526.

[5] a) B. W. Smith, M. Monthioux, D. E. Luzzi, *Nature* **1998**, *396*, 323; b) B. W. Smith, D. E. Luzzi, *Chem. Phys. Lett.* **2000**, *321*, 169; c) N. Nakashima, Y. Tanaka, Y. Tomonari, H. Murakami, H. Kataura, T. Sakaue, K. Yoshikawa, *J. Phys. Chem. B* **2005**, *109*, 13076.

[6] a) K. Hirahara, K. Suenaga, S. Bandow, H. Kato, T. Okazaki, H. Shinohara, S. Iijima, *Phys. Rev. Lett.* **2000**, *85*, 5384; b) T. Shimada, T. Okazaki, R. Taniguchi, T. Sugai, H. Shinohara, K. Suenaga, H. Ohno, S. Mizuno, S. Kishimoto, T. Mizutani, *Appl. Phys. Lett.* **2002**, *81*, 4067; c) Y. Maeda, S. Kimura, Y. Hirashima, M. Kanda, Y. Lian, T. Wakahara, T. Akasaka, T. Hasegawa, H. Tokumoto, T. Shimizu, H. Kataura, Y. Miyauchi, S. Maruyama, K. Kobayashi, S. Nagase, *J. Phys. Chem. B* **2004**, *108*, 18395.

[7] Y.-B. Sun, Y. Sato, K. Suenaga, T. Okazaki, N. Kishi, T. Sugai, S. Bandow, S. Iijima, S. Shinohara, *J. Am. Chem. Soc.* **2005**, *127*, 17972.

[8] a) D. A. Britz, A. N. Khlobystov, J. Wang, A. S. O'Neil, M. Poliakoff, A. Ardavan, G. D. Briggs, *Chem. Commun.* **2004**, 176; b) D. A. Britz, A. N. Khlobystov, K. Porfyrakis, A. Ardavan, G. D. Briggs, *Chem. Commun.* **2005**, 37.

[9] R. S. Lee, H. J. Kim, J. E. Fischer, A. Thess, R. E. Smalley, *Nature* **1997**, *388*, 255.

[10] R. R. Meyer, J. Sloan, R. E. Dunin-Borkowski, A. I. Kirkland, M. C. Novotny, S. R. Bailey, J. L. Hutchison, M. L. H. Green, *Science* **2000**, *289*, 1324.

[11] a) M. Kalbac, L. Kavan, M. Zukalova, L. Dunsch, *J. Phys. Chem. B* **2004**, *108*, 6275; b) L. H. Guan, K. Suenaga, Z. J. Shi, Z. N. Gu, S. Iijima, *Phys. Rev. Lett.* **2005**, *94*, 045502.

[12] G. Hummer, J. C. Rasaiah, J. P. Noworyta, *Nature* **2001**, *414*, 188.

[13] S. Okada, S. Saito, A. Oshiyama, *Phys. Rev. Lett.* **2001**, *86*, 3835.

[14] D. J. Hornbaker, S.-J. Kahng, S. Misra, B. W. Smith, A. T. Johnson, E. J. Mele, D. E. Luzzi, A. Yazdani, *Science* **2002**, *295*, 828.

[15] J.-F. Nierengarten, V. Gramlich, F. Cardullo, F. Diederich, *Angew. Chem.* **1996**, *108*, 2242; *Angew. Chem. Int. Ed. Engl.* **1996**, *35*, 2101, and references therein.

[16] P. R. Ashton, D. W. Anderson, C. L. Brown, A. N. Shipway, J. F. Stoddart, M. S. Tolley, *Chem. Eur. J.* **1998**, *4*, 781.

[17] B. Y. Lee, M. Miller, *J. Org. Chem.* **1983**, *48*, 24.

[18] S. Zhang, Y. Rio, F. Cardinali, C. Bourgogne, J.-L. Gallani, J.-F. Nierengarten, *J. Org. Chem.* **2003**, *68*, 9787, and references therein.

[19] D. M. Guldi, G. N. A. Rahman, J. Ramey, M. Marcaccio, D. Paolucci, F. Paolucci, S. Qin, W. T. Ford, D. Balbinot, N. Jux, N. Tagmatarchis, M. Prato, *Chem. Commun.* **2004**, *18*, 2034.

[20] D. M. Guldi, G. M. A. Rahman, S. Qin, M. Tchoul, W. T. Ford, M. Marcaccio, D. Paolucci, F. Paolucci, S. Campidelli, M. Prato, *Chem. Eur. J.* **2006**, *12*, 2152.

[21] M. A. Herranz, F. Diederich, L. Echegoyen, *Eur. J. Org. Chem.* **2004**, 2299.

[22] C. Bruno, I. Doubitski, M. Marcaccio, F. Paolucci, D. Paolucci, A. Zaopo, *J. Am. Chem. Soc.* **2003**, *125*, 15738.

[23] C. Boudon, J.-P. Gisselbrecht, M. Gross, L. Isaacs, H. L. Anderson, R. Faust, F. Diederich, *Helv. Chim. Acta* **1995**, *78*, 1334.

[24] D. M. Guldi, M. Marcaccio, F. Paolucci, D. Paolucci, J. Ramey, R. Taylor, J. A. Burley, *J. Phys. Chem. A* **2005**, *109*, 9723.

[25] C. Ehli, G. M. A. Rahman, N. Jux, D. Balbinot, D. M. Guldi, F. Paolucci, M. Marcaccio, D. Paolucci, M. Melle-Franco, F. Zerbetto, unpublished results.

[26] a) R. B. Martin, K. F. Fu, Y.-P. Sun, *Chem. Phys. Lett.* **2003**, *375*, 619; b) T. Gareis, O. Kothe, J. Daub, *Eur. J. Org. Chem.* **1998**, 1549; c) I. B. Martini, B. Ma, T. Da Ros, R. Helgeson, F. Wudl, B. J. Schwartz, *Chem. Phys. Lett.* **2000**, *327*, 253; d) K. Kordatos, T. Da Ros, M. Prato, C. Luo, D. M. Guldi, *Monatsh. Chem.* **2001**, *132*, 63; e) F. Hauke, A. Hirsch, S. Atalick, D. M. Guldi, *Eur. J. Org. Chem.* **2005**, 1741.

[27] D. M. Guldi, M. Prato, *Acc. Chem. Res.* **2000**, *33*, 695.

[28] D. M. Guldi, G. M. A. Rahman, N. Jux, D. Balbinot, U. Hartnagel, N. Tagmatarchis, M. Prato, *J. Am. Chem. Soc.* **2005**, *127*, 9830.

[29] M. Carano, P. Ceroni, L. Mottier, F. Paolucci, S. Roffia, *J. Electrochem. Soc.* **1999**, *146*, 3357.

Received: January 25, 2006
Published online: April 3, 2006

